

Investigation of Microstructure And Mechanical Properties of Al-Zn-Mg and Al-Zn-Mg-Sc Alloys After Double Passes Friction Stir Processing

P. K. Mandal*

Department of Metallurgical & Materials Engineering, Indian Institute of Technology Roorkee (IITR), Roorkee, Uttarakhand, India.

* Corresponding author. Tel.: +91-9045632268; e-mail: pkmmet@yahoo.in

Manuscript submitted January 10, 2017; accepted March 28, 2017.

doi: 10.17706/ijmse.2017.5.2.47-59

Abstract: In this study, the two types of aluminium alloys namely Al-Zn-Mg and Al-Zn-Mg-Sc were developed by casting route. The cast plates were subjected to double passes friction stir processing (FSP) by in-situ vertically fitted milling machine. The tool design and process parameters were found to affect the microstructural and mechanical properties of these aluminium alloys. Therefore, the experimental samples were collected from the stirring zone and selected for mechanical testing. The FSP caused intense plastic deformation, material mixing, and thermal exposure, resulting in significant microstructural refinement, densification, and homogeneity of processed zone. It has been observed that the mechanical properties improved as a result of the complex interactions due to FSP, thermo-mechanical effects, dissolution, coarsening and re-precipitation of the strengthening precipitates in these two experimental aluminium alloys. It can be concluded that the strengthening effect of the Al-Zn-Mg and Al-Zn-Mg-Sc alloys after FSP are associated with the fine grain strengthening, subgrain strengthening and precipitation strengthening of Al_3Sc and $MgZn_2$ precipitates. Finally, the resultant properties have been evaluated by FSP parameters such as rotational speed of 1000 rpm and traverse speed of 70 mm/min and specified tool design. In addition, the detrimental effect of high Zn content (~8.20 wt.%) and high Sc content (~0.87 wt.%) aluminium alloy may be attributed to the vaporization of Zn at the time of the FSP. The experimental samples were collected from double passes FSPed zone and critically examined for optical microscopy (OM), scanning electron microscopy (SEM), field emission scanning electron microscopy (FESEM), transmission electron microscopy (TEM), Vicker's hardness testing, tensile testing and fractographic analysis.

Keywords: Double passes FSP, Al_3Sc particles, Zn vaporization, fractographic analysis.

1. Introduction

The Al-Zn-Mg and Al-Zn-Mg-Sc alloys are exhibited age-hardening effects and good mechanical properties. Scandium (Sc) used for grain refinement agent in cast aluminium alloys [1]-[3]. The main functions of these alloys are to increase strength without affecting other properties. The Zn/Mg ratio is the major criterion to formation of main precipitates (η for Zn/Mg >2 or T for Zn/Mg <2) of age-hardening alloys. The peak hardness is increased with increasing Zn/Mg ratio. The particles η , η' and Al_3Sc are the main stages involved in 7xxx series aluminium alloys [4]-[6]. Impurity elements like Fe and Si are formed intermetallic compounds and degrade the fracture toughness properties. Moreover, solution treatment at 465°C for 1h then immediately water quenching (T_4) reduces the cast inhomogeneity, grain boundary segregation and

dissolve inclusions like η (MgZn_2) and $T(\text{Al}_2\text{Zn}_3\text{Mg}_3)$ phases in the temperature range 435-445°C in the matrix [7]. Loss of thermal conductivity is significantly degraded by multiply alloying precipitation hardening elements such as Mg, Fe, and Si [8], [9]. FSP is the advanced solid state technique to modify cast surface layers and to enhance specific properties to some considerable depth. Although, the basic principle is based on FSW (friction stir welding). FSW was first developed at The Welding Institute (TWI) in Cambridge, UK in 1991 [10], [11]. This process is particularly suitable for welding/processing of non-ferrous metals with low melting points such as magnesium, aluminium, brass, titanium, zinc and lead. Because of melting does not occur and processed area takes place below the melting point ($\sim 0.6-0.8$ of T_m) of the base material, a good quality of processed or weld zone is created. The heat input during FSP creates from friction and plastic deformation which indicates FSP is a green and energy-efficient technique without harmful gas, radiation and noise. The component shape and size is remaining same after FSP. A specially designed cylindrical tool, consisting of a shoulder and a profiled pin is inserted into the work piece by a rotational movement with the axial force. A temperature rise of 400°C to 500°C has been reported within the SZ (stir zone) of Al-Zn-Mg alloys [12], [13]. Main parameters have been too applied such as rotational speed, traverse speed and specific tool design. It is also well understood that the effect of these important parameters on the FSP properties are the major topics for researchers. Obviously, FSP parameters were selected by trial and error to fix the process to obtain sound and defects free materials. FSP achieved three distinct zones, namely as nugget or SZ (stir zone), TMAZ (thermo-mechanically affected zone) and HAZ (heat affected zone) due to the stirring action of a rotating tool with axial force and the plate travel speed [14]. FSP causes grain refinement due to the dynamic recrystallization in the SZ which increase the tensile properties without loss of ductility [15]. According to Mishra *et al.* (2000) has been reported that the Al-Zn-Mg alloys subjected to FSP exhibits superplastic formation at a 480°C and the thermal stability of refined grains achieved during FSP at around $\sim 500^\circ\text{C}$ [16]. This is considering a high temperature process when fine-grains formed during FSP grow rapidly under the influence of thermal cycles in air cooling. Thus, FSP Al alloys results in the formation of a homogeneous fine grained structure at around $\sim 1-10 \mu\text{m}$ which have developed high angle grain boundaries about $\sim 80-90\%$. Notably, the grain refinement caused by secondary Al_3Sc nanoparticles, precipitation strengthening and sub-grain strengthening mechanisms. The presence of such nanoparticles or dispersoids is known to restrict the grain growth through Zener pinning [17]. The present work has two highlights on some deleterious effects like Zn vaporization due to high rotational speed of 1000 rpm and traverse speed of 70 mm/min and formation of Al_3Sc chunky particles due to high Sc (0.87 wt.%) content in aluminium alloys. Such defects have been identified through OM, FESEM, TEM and SEM fractographs analysis. Investigations determine the mechanical properties should be optimized when process parameters are avoided to Zn vaporization or hair line crack forming on the stir region during FSP [18]. The present research has to determine the effects on microstructure and mechanical properties under T_4 +FSP and T_4 +FSP+Aged at 140°C for 2h conditions of the 7xxx series of Al-Zn-Mg alloys.

2. Experimental Procedure

The present experimental works were carried out on aluminium alloys through cast metallurgy route and alloy compositions were tested by ICP-AES and AAS methods shown in Table 1. The physical and thermal properties of aluminium alloys are mentioned in Table 2. In general, thermal conductivity depends on solute content, while Mg content increasing with thermal conductivity decrease. The evolution of microstructure was investigated by optical microscopy (OM), field emission scanning electron microscopy (FESEM), transmission electron microscopy (TEM) and scanning electron microscopy (SEM) tensile fractographs analysis. The properties of the prepared aluminium alloys were evaluated at T_4 , T_6 , T_4 +FSP and T_4 +FSP+Aged at 140°C for 2h conditions, respectively. The metallographic specimens were collected from

as-cast plate and subjected to solution treatment at 465°C for 1h and immediately quenched in water (T₄). Similarly, sample was collected from FSP region and mechanically polished using different grades of emery papers with the help of rotating wheel using water + Al₂O₃ powder. Final polishing was done using diamond paste with particle size of 1-2 μm in the separate rotating wheel. Then the samples were etched by using Keller's reagent (1%HF + 1.5%HCl + 2.5%HNO₃ + 95%H₂O, volume fraction) for reveal microstructures. The T₄ sample was selected for artificial ageing treatment.

Table 1. Chemical Composition (in wt.%) of Studied Aluminium Alloys

Alloy no.	Zn	Mg	Sc	Si	Fe	Al	Zn+Mg	Zn/Mg
1	8.34	3.30	-	0.02	0.04	Bal.	11.64	2.53
2	8.20	5.70	0.87	0.88	0.42	Bal.	13.90	1.44

Table 2. Physical and Thermal Properties of Al-Zn-Mg Alloy

Density (g/cc)	2.72
Melting point (°C)	652
Modulus of elasticity (GPa)	68.9
Poisons ratio	0.33
Thermal conductivity (W/m-K)	167
Thermal diffusivity (m ² /s)	5.37 × 10 ⁻⁵
Specific heat capacity (J/g/°C)	0.869

Table 3. FSP Tool Characteristics and Process Parameters

Shoulder diameter (mm)	20
Pin diameter (mm)	3
Pin height (mm)	3.5
Clockwise and unidirectional, tool rotational speed (rpm)	1000
Tool traverse speed (mm/min)	70
Downward pressure (kN)	15
Tool tilt angle (°)	2.5
Number of passes	two
Plate dimension	150×90×8 mm ³

The artificial ageing was performed in electrical resistance muffle furnace with precision controlled temperature at 140±2°C. The ageing kinetics was characterized through Vicker's hardness tester (FIE VM50 PC) with 10 kg. load at 15 sec dwell time of aluminium alloys. The two types of FSP samples were collected such as T₄+FSP and T₄+FSP+Aged at 140°C for 2h and stored for different types of testing. Differential scanning calorimetry (DSC) was performed on the EXSTAR TG/DTA 6300 equipment with a heating rate 10°C/min. The FESEM micrograph with EDAX analysis was presented at T₄+FSP+Aged at 140°C for 2h condition of aluminium alloys. The transmission electron microscope (TEM) analysis was performed using twin-jet electro-polishing (solution was 75% CH₃OH and 25% HNO₃) at 12 V and -35 °C. All the imaging was carried out using at Techai G² 20 S-TWIN at 200 kV. The hardness measurements of specimens were investigated by Vicker's macrohardness tester under a load of 10 kg. on the perpendicular to the FSP direction. The specimens for tensile tests were cut in the longitudinal direction parallel to the direction of processing. The dimensions of tensile sample (ASTM: E-8/E8M-11sub-size) has shown in Fig. 1(c). The process parameters were kept on constant at every unidirectional pass of FSP of 1000 rpm and 70 mm/min as shown in Table 3. The mechanical testing was carried out an electro-mechanically controlled universal testing machine (25 kN, H25 K-S, UK) with cross head speed 1 mm/min after FSP and results are calculated and exhibited at bar diagrams format in Fig. 10.

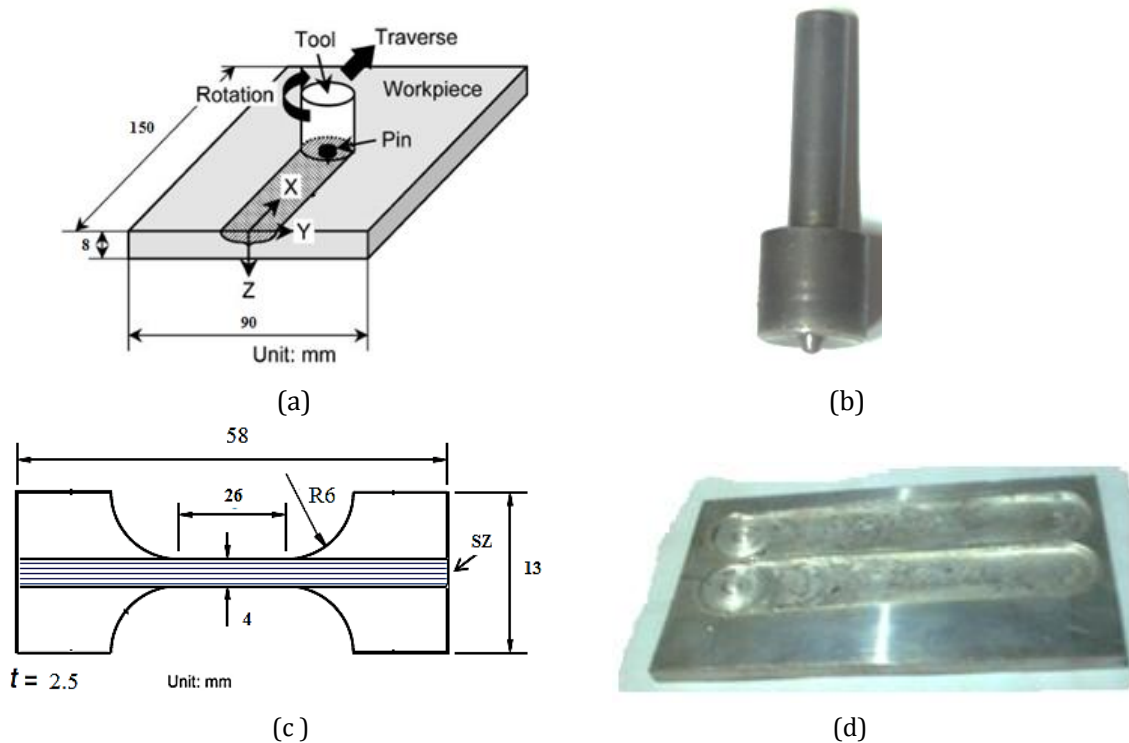


Fig. 1 (a) Schematic diagram of FSP set-up ($150 \times 90 \times 8$ mm³), (b) Illustration of tool configuration, (c) Geometry and dimensions of the tensile test sample, (d) Illustration of double passes FSP plate ($150 \times 90 \times 8$ mm³).

3. Results and Discussion

The Al-Zn-Mg is a novel alloy with light weight, high specific strength and good mechanical properties. A little amount of Sc utilized in alloys with specific control even with a little variation possibly may have a great impact on material performance. Zn and Mg elements also cause of quench sensitivity, which is the premature precipitation of coarse η particles and it reduced by Sc addition [19]. Thus, conductivity is an indirect measurement of the phase transformation which indication of the type, size and amount of precipitates formation in aluminium alloys. The aluminium alloy in the solutionizing (T_4) state has the lowest conductivity due to the decrease of the mean free path of electrons. The main mechanisms are mismatch of sizes between the solute and solvent atoms, and the electron/atom ratio in solid solution is different completely [20]. Many researchers were suggested on the FSP of engineering alloys to promote process windows which have been applied in the industrial application effectively [21], [22]. These alloys can be used in many applications such as cylinder heads, engine blocks, aerospace housings, gear pumps, aircraft fittings, general automotive castings, and marine structures [23]. Sc has been found to result in grain refinement through the eutectic form at 655°C of Al_3Sc compound favours the nucleation of aluminium grains while Ti, V, Cr forms peritectic with aluminium. The primary particles (Al_3Sc) are formed in different shapes in different cooling rate, which act as a grain refining of aluminium alloys. Grain refinement by Sc inoculation has been commonly used to improve the mechanical properties of aluminium alloys. It is fact that increase in Sc initially strength increases, however more than 0.6 wt.% mechanical properties remain same. Sc is the costlier element and it can substitute by other rare earth elements and higher order alloy combination. The addition of Mg in binary Al-Sc alloys has been shown to form primary particles (Al_3Sc) much lower that the eutectic composition of Sc in such aluminium alloys [24]. Mg improves the mechanical properties through solid solution strengthening. There is extensive investigation reported

on cubic Al_3Sc particles (melting point of 1320°C). Comparative study is reported on crystallographic mismatch between Al & Al_3Sc ($\sim 1.5\%$) is higher than between Al & Al_3Ti ($\sim 1.18\%$) and Al & Al_3Zr ($\sim 0.7\%$) in some specific crystallographic plane and room temperature [25], [26]. Fig. 2 indicates the existence of four phases equilibrium in this system, in which the $\alpha\text{-Al}$, $\eta(\text{MgZn}_2)$, $\tau(\text{Al}_2\text{Mg}_3\text{Zn}_3)$, and Al_3Sc phases are involved [27].

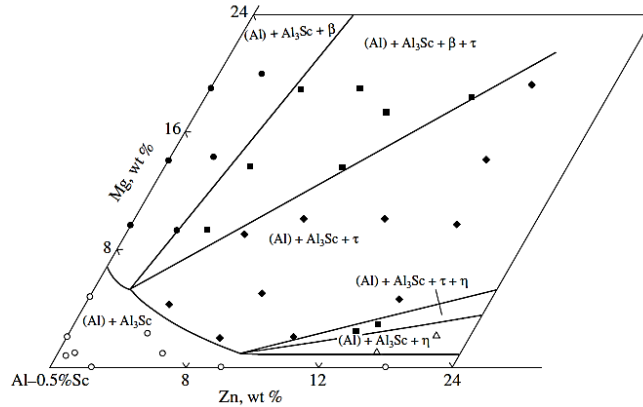


Fig. 2. Section of the isothermal tetrahedron of the Al-Zn-Mg-Sc system (300°C) [28].

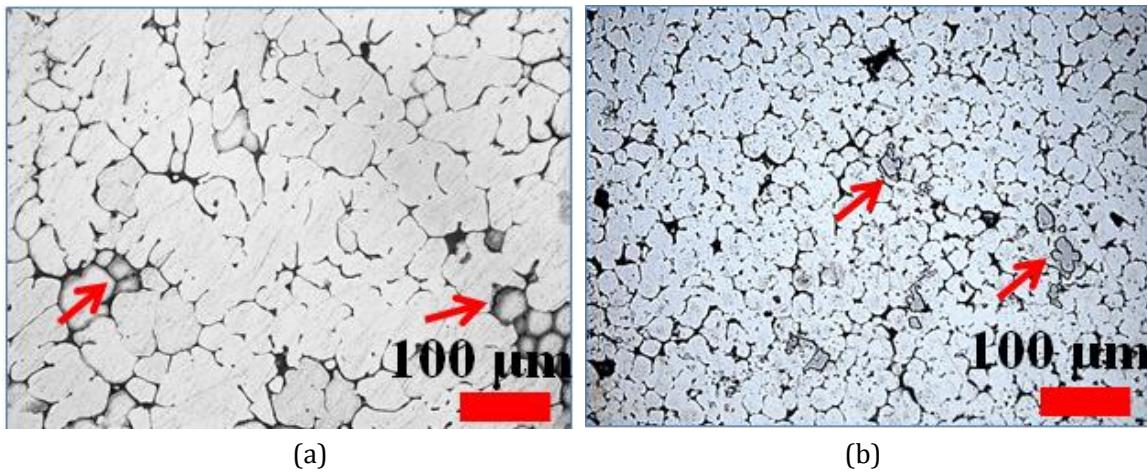


Fig. 3. Optical micrographs of as-cast aluminium alloys (T4 condition): (a) Alloy-1, (b) Alloy-2.

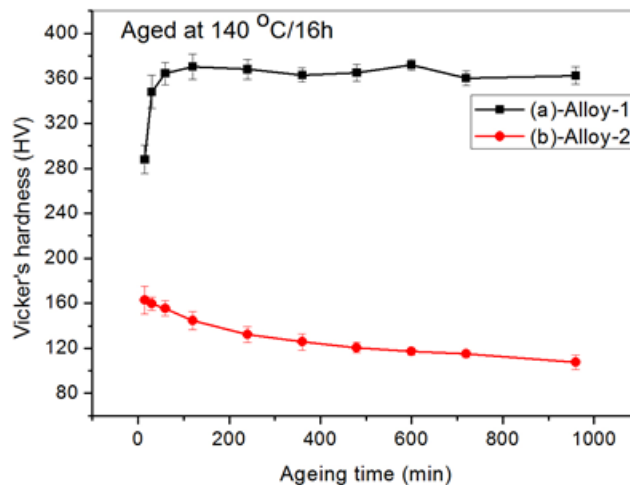


Fig. 4. Illustration of ageing curves of aluminium alloys (T_6): (a) Alloy-1, (b) Alloy-2.

Fig. 3 shows T₄ alloys exhibited grain boundary segregation with black spots on the boundary regions. Due to high solute contents (11.64 wt.%) prone to segregation of eutectic constituents on the grain boundaries as shown in Fig. 3(a). Fig. 3(b) shows Al₃Sc chunky particles and several black spots on the grain boundaries owing to high Sc content (0.87 wt.%) and high solute content (13.90 wt.%), respectively. Since, both of the alloy constituents are very high levels, so present solution treatment (465°C for 1h) may not be feasible to optimum dissolve second phases in the matrix.

Fig. 4 shows ageing curve of T₄ alloys. The maximum hardness values developed by age-hardening alloys can be attributed to precipitation of coherent and finely dispersed η -MgZn₂ phases as foreign atom in the lattice of the solvent atoms in the solid solution. These are the main causes of more lattice distortion to make alloys harder. Elements like Zn and Mg are the substitutional atoms in aluminium matrix produced elastic lattice distortions by solid solution strengthening. Hence, the main strengthening mechanisms exhibited in these alloys are an age-hardening by structural precipitates of MgZn₂ formed during artificial ageing treatment. These precipitate fine particles act obstacles to dislocation movement and thereby strengthen the Al-Zn-Mg alloy [29]. Fig. 4(a) shows ageing curve exhibited maximum hardening effects at around 100 min ageing time due to high solute content produce high density of η -MgZn₂ particles with optimum size in this ageing treatment regime. Fig. 4(b) shows ageing curve exhibited minimum hardening effects due to high Sc content produce Al₃Sc chunky particles or agglomeration tendency of Al₃Sc particles aggravated with high solute content in this ageing treatment regime.

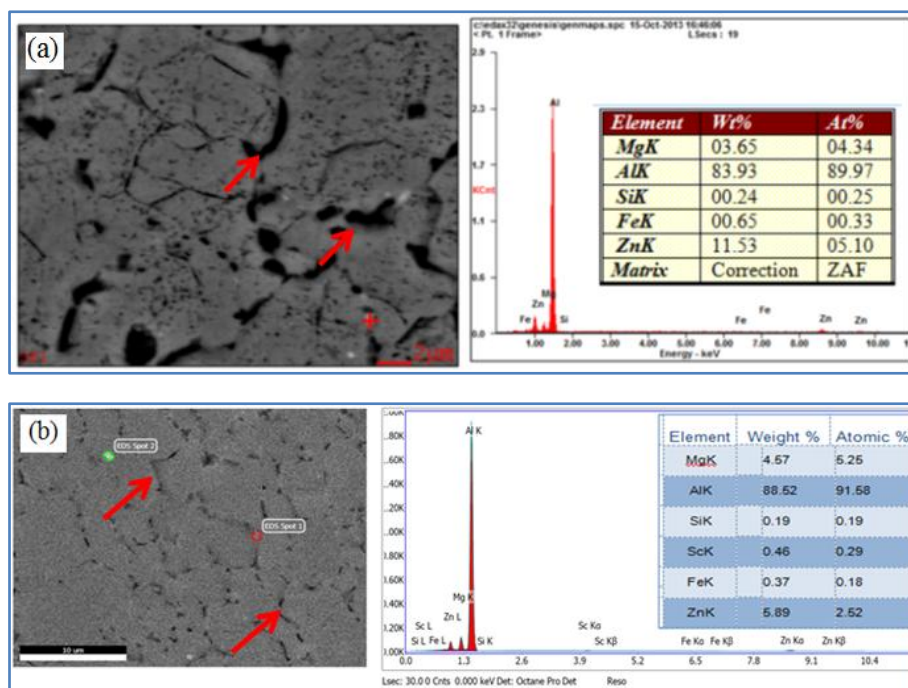


Fig. 5. The FESEM micrographs exhibiting black holes with EDAX analysis at T₄+FSP+Aged at 140°C/2h condition: (a) Alloy-1, (b) Alloy-2. (1000 rpm and 70 mm/min).

Fig. 5 shows FESEM micrograph with EDX analysis after T₄+FSP+Aged at 140°C for 2h condition. Fig. 5(a) shows FESEM micrograph exhibited several black spots (indicated by red arrows) indicate Zn vaporization may be occurred due to high heat generation (~550°C) during FSP. This deleterious effect main causes of low mechanical properties of FSP aluminium alloy. Fig. 5(b) shows FESEM micrograph exhibited formation of grain boundaries with continuous network of black lines (indicated by red arrows) may be same reason

like Zn vaporization aggravated with high density of Al_3Sc particles during FSP aluminium alloy.

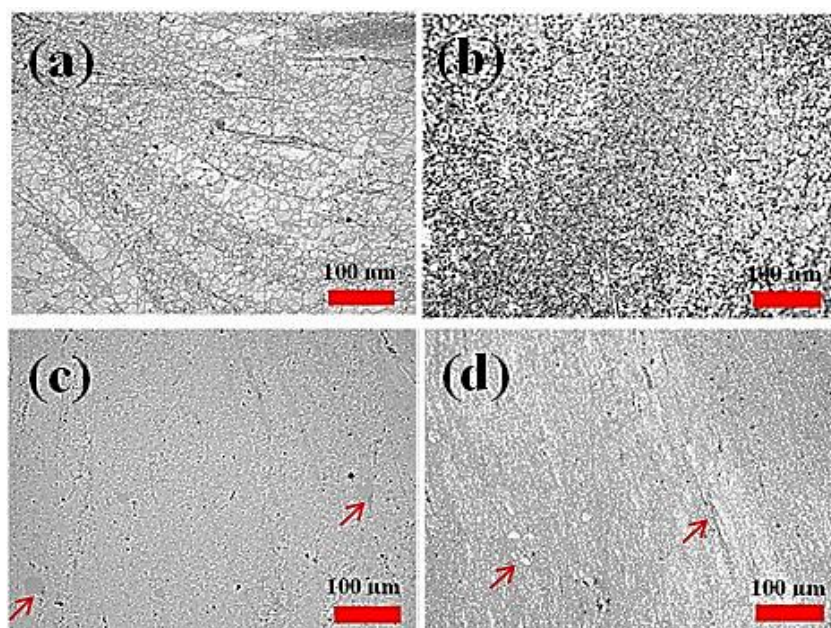


Fig. 6. Illustration of optical micrographs collected from SZ for Alloy-1 at (a) T_4 +FSP, (b) T_4 +FSP+Aged at $140^\circ\text{C}/2\text{h}$ condition; for Alloy-2 at (c) T_4 +FSP, (d) T_4 +FSP+Aged at $140^\circ\text{C}/2\text{h}$ condition. (1000 rpm and 70 mm/min).

Fig. 6(a) shows optical micrograph exhibited fine and equiaxed grains of SZ after T_4 +FSP condition of Alloy-1. The microstructure of present alloy consists of equiaxed grains that can be induced during the dynamic recrystallization process. It is well known the FSP generates substantial fictional heat and intense plastic deformation for creating fine recrystallized grains in the SZ. Therefore, the FSP improves the grain boundary formation and increases suitable sites for the precipitation of nucleation in post ageing treatment at 140°C for 2h as shown in Fig. 6(b). Fig. 6(c) shows the optical micrograph exhibited several chunky particles (marked by red arrows) even after T_4 +FSP condition. Also, some fine cracks are exhibited due to FSP torsional effects could not be resisting such cracks as presence of coarse Al_3Sc particles. Both the causes are pertinent of high Sc content (0.87 wt.%) due to formation of Al_3Sc chunky particles as proven by TEM analysis and mechanical properties. In case of post ageing treatment at 140°C for 2h for Alloy-2 (Fig. 6.d) exhibited fast coarsening effects due to Al_3Sc chunky particles and high Zn content (8.20 wt.%) formed high fraction of high angle of grain boundaries, high mobility of atoms would affect its thermal stability adversely during FSP. These types of Al_3Sc chunky particles are unable to the pinning action to refine grains by Zener drag mechanism. Moreover, dynamic grain growth mechanism is prominent rather than recrystallization process. There are three types of adverse effects have been postulated such as hair line cracks generation, several black spots due to Zn vaporization, and several Al_3Sc chunky particles formation (all marked by red arrows). The DSC curve of the experimental alloys in the present state is presented in Fig. 7. The DSC curves show the main two transition points at around 475°C - 510°C (exothermic reaction) and 615°C - 620°C (endothermic reaction), respectively. Two alloys show the similar trend and almost the reaction temperature (475°C - 510°C) in this state, which indicates that the combined effects of high Zn content and high Sc content main causes of formation of high density of Al_3Sc particles and η - MgZn_2 phases exhibit anti-recrystallization effects. The endothermic reaction (615°C - 620°C) is mainly caused by the formation and growth Al_3Sc particles and dissolution of η phases and melting reaction of $T(\text{Al}_2\text{Mg}_3\text{Zn}_3)$ phases. The precipitate characteristics in the experimental alloys have been shown in the TEM analysis in

Fig. 8. It is observed that the precipitates in the post ageing treatment at 140°C for 2h alloy have a coarse and spherical shapes and an average grain size ~20-45 nm as shown in Fig. 8(a). Some of needle shape precipitates are long size ~130-200 nm. Due to post ageing at 140°C for 2h, homogeneous nucleation sites are activated in the matrix and consequently the precipitated can be formed in the mostly spherical shape within the matrix with a uniform distribution. The high solute content (11.64 wt.%) with high temperature generates during plastic deformation are the main causes of formation of coarse MgZn₂ precipitates. This is attributed to the loss of metastable age-hardening precipitates and the formation of equilibrium η precipitates during FSP, which reduced the precipitation hardening contribution [30], [31].

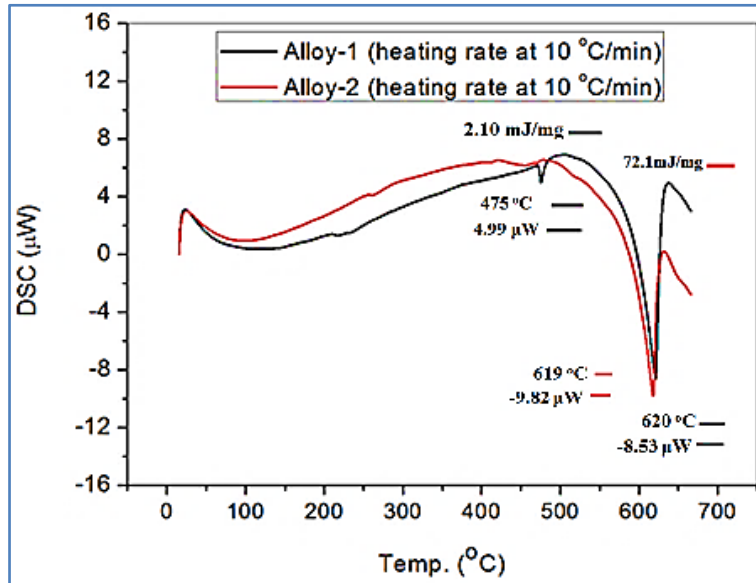


Fig. 7. DSC analysis of aluminium alloys at T₄+FSP+Aged at 140°C/2h condition. (1000 rpm and 70 mm/min)

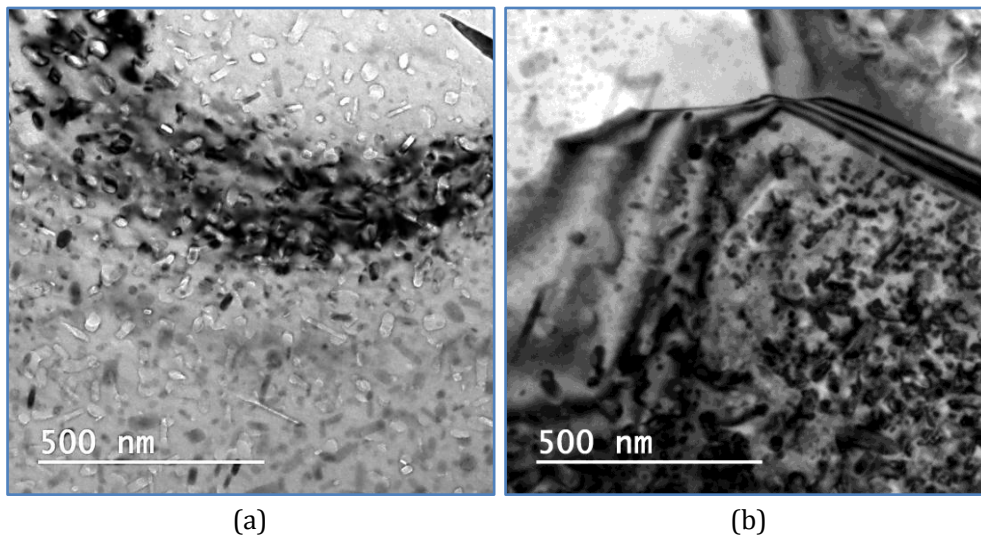


Fig. 8. TEM micrographs collected from SZ of aluminium alloys at T₄+FSP+Aged at 140°C/2h condition: (a) Alloy-1, (b) Alloy-2. (1000 rpm and 70 mm/min).

Fig. 8(b) shows TEM micrograph exhibited different shapes and morphology of precipitates after Sc addition of Al₃Sc precipitates. Fine and coarse mixture type coherent spherical Al₃Sc particles appear in Alloy-2 after T₄+FSP+Aged at 140°C for 2h. These particles had strong interaction with the dislocations and the grain boundaries during FSP. Some of precipitates are big size ~120-200 nm. This is because

agglomeration tendency among the coarse precipitates of high solute atoms and high density of Al_3Sc particles facilitated during FSP. Appearance of long dislocation line introduced into the FSP alloy. Since aluminium has high stacking fault energy, so the presence of dislocations suggest that recrystallization was not complete and that it had a more dynamic nature than static character. The refinement of microstructure during FSP is an inherent feature of the process. It is usually considered as a result of dynamic recrystallization accompanying FSP. The results revealed the $\eta(MgZn_2)$ phases precipitated around the Al_3Sc particles to reduce the oversaturated degree of solute atoms in the matrix [32]-[34]. Hence, the effect of precipitate strengthening has not obvious and the strength of Alloy-2 is lower than that of Alloy-1 as shown in Fig. 10.

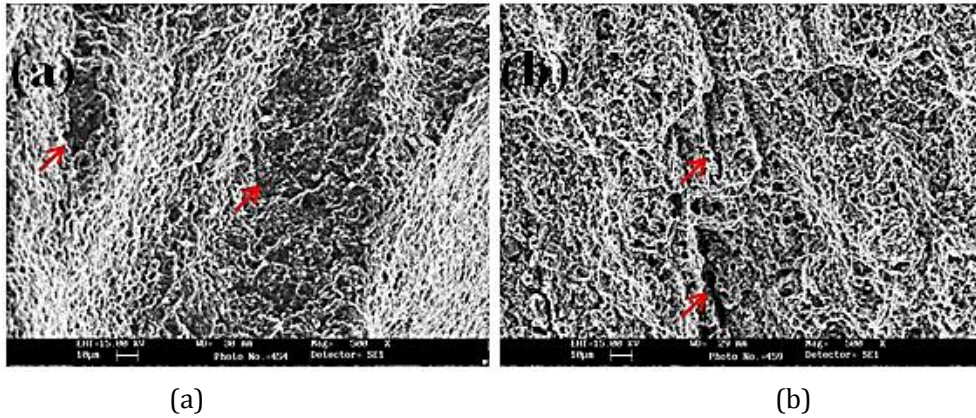


Fig. 9. SEM tensile fractographs at T₄+FSP+Aged at 140°C/2h condition: (a) Alloy-1, (b) Alloy-2. (1000 rpm and 70 mm/min).

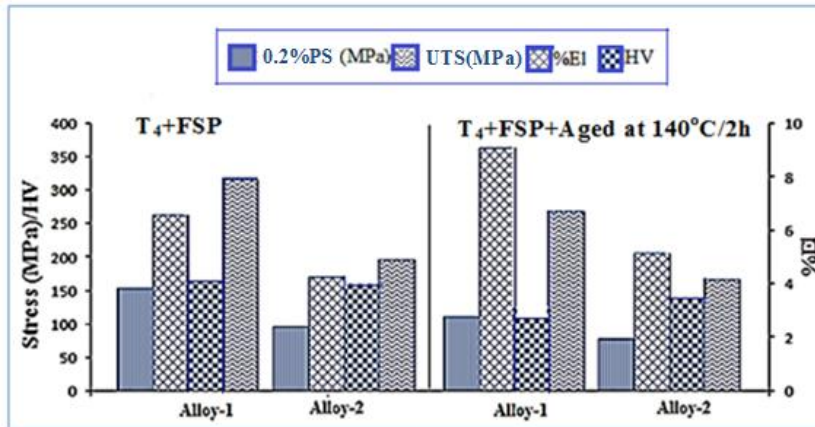


Fig. 10. Illustration of bar diagrams of mechanical properties at different conditions of Al-Zn-Mg alloy after double passes FSP. (1000 rpm and 70 mm/min).

In Fig. 9 shows tensile fractographs exhibited ductile manner of entire fracture surface for both the alloys at the present condition. In Fig. 9(a) shows several black holes/cracks (indicated by red arrows) seems stress raiser points created by Zn vaporization during FSP (causes for high heat input; where, heat input = rpm/traverse speed = 1000/70 = 14.39). Fig. 9(b) shows several crack lines (indicated by red arrows) which may have generated along the Al_3Sc chunky particles or Zn vaporization points, also, accelerated after post ageing treatment at 140°C for 2h. Formation of Al_3Sc chunky particles (for 0.87 wt.% Sc content) facilitated due to high angle grain boundaries (generally 80-90%) during FSPed. It is observed that the mechanical

properties are a result of the complex interactions between FSP the thermo-mechanical effects and the processes of dissolution, coarsening and reprecipitation of the strengthening precipitates in these aluminium alloys as shown in Fig. 10. In both the processing conditions, the mechanical properties have been enhanced due to fine grains and eliminated porosities and $\eta(\text{MgZn}_2)$, Al_3Sc particles dispersive action. The precipitation strengthening is the main mechanism in association of nano-scale precipitates (η , Al_3Sc) and its precursors. Also, microstructural analysis stated that it has to major attribution due to dynamic recrystallization in SZ. Thus, the FSP enhances the grain boundary formation and increases suitable sites for the precipitation of nucleation in post ageing treatment. Also, extended the hardening effects due to fine precipitates at the grain boundary of ultrafine grained aluminium alloys. Since the mechanical properties such as hardness and strength of alloys are related to the grain size and according to Hall-Petch equation, the hardness ($\sim 175\text{HV}$) in SZ increases remarkably. Specially, after post ageing treatment all mechanical properties are diminished except %elongation of Alloy-1. In contrary, high Zn content (8.20 wt.%) and high Sc content (0.87 wt.%) of Alloy-2 exhibited lower mechanical properties in both the cases. It is clearly indicated that the formation of Al_3Sc chunky particles and $\text{T}(\text{Al}_2\text{Zn}_3\text{Mg}_3)$ precipitates as observed in optical micrographs of Al-Zn-Mg alloy (Alloy-1) and Al-Zn-Mg-Sc alloy (Alloy-2) in Fig. 6(c-d).

4. Conclusions and Future Trends

From the work presented in this paper the following conclusions can be drawn for aluminium alloys. The latest development in FSW/FSP research has been concentrated on expanding the usefulness of this procedure for ferrous alloys (e.g. carbon steels or stainless steels) or high temperature nickel-based alloys, by developing special tools that can sustain high temperature and pressure needed to join these metals. Many advantages using FSP are mention likely to transform a heterogeneous microstructure to homogeneous refined microstructure, form nanostructure surface as a result increases the hardness of the alloys, and to improve the tensile properties of the surface materials. In addition, high Zn (8.20 wt.%) and high Sc (0.87 wt.%) content of Al-Zn-Mg alloys in connection with FSP (with optimum process parameters) may result in improved mechanical properties, which is need to be explored.

- 1) The maximum ageing hardness ($\sim 370\text{HV}$) of the Al-Zn-Mg alloy (Alloy-1 in Fig. 4) is believed to enhance mainly from the presence of the fine dispersion of η particles, which are most probably coherent in the matrix.
- 2) FSP is a novel surface modification technique and resulted in substantial grain refinement with numerous commercial applications of Al-Zn-Mg alloys. In the present task, the whole characterizations have been done by double passes FSP under precise controlled process parameters.
- 3) FSP created three distinct zones namely as stir zone (SZ), thermo-mechanically affected zone (TMAZ) and heat affected zone (HAZ) due to the stirring action of a rotating tool with axial force and the plate travel speed. SZ comprises very fine and recrystallized grains primarily due to severe plastic deformation and dynamic recrystallization.
- 4) The TEM micrographs at low and high magnifications have revealed that Sc added and T_4 +FSP+Aged at 140°C for 2h alloys, contain $\eta(\text{MgZn}_2)$ and Al_3Sc precipitates which are fully coherent, well-distributed, thermodynamically stable and very effective in stabilizing the fine microstructure. Because of intense plastic deformation and elevated temperature (450°C - 500°C) in the SZ, microstructure exhibited fine recrystallized grains with predominant high angle grain boundaries and Al_3Sc coarse particles in the matrix. Due to high Zn content (8.20 wt.%) and high Sc content (0.87 wt.%) the coarsening tendency of η , $\text{T}(\text{Al}_2\text{Zn}_3\text{Mg}_3)$ and Al_3Sc precipitates increased. It is also clearly observed that for non-Sc Al-Zn-Mg alloys, after FSP microstructure showed finer grains and the high density of second-phase finely distributed precipitates enhance mechanical properties.

- 5) The tensile fractographs revealed Al₃Sc chunky particles, the source of crack formation which might be the reason for low tensile properties. Even after FSP these particles were found to be source of crack initiation.
- 6) The tensile properties have been evaluated for T₄+FSP and T₄+FSP+Aged at 140°C for 2h conditions. The tensile properties of Alloy-1 decreased marginally such as ultimate tensile strength of 14.77%, 0.2% proof strength of 26.74%, hardness of 30.42%, but elongation increase of 37.88% after T₄+FSP+Aged at 140°C for 2h. Similarly, the tensile properties of Alloy-2 increased marginally such as ultimate tensile strength of 5%, 0.2% proof strength of 15%, elongation of 19%, but decreased hardness of 6.3%, after T₄+FSP+Aged at 140°C for 2h. Reason for increased strength during post ageing treatment effects of fine nucleation of MgZn₂ homogeneous precipitates and fine grains, fragmentation of Al₃Sc dispersoids through Orowan mechanism.

References

- [1] Deng, Y., Yin, Z. M., Zhao, K., Duan, J. Q., & He, Z. B. (2012). Effects of Sc and Zr microalloying additions on the microstructure and mechanical properties of new Al-Zn-Mg alloys. *Journal of Alloys and Compounds*, 530(7), 71-80.
- [2] Hyde, K. B., Norman, A. F., & Prangnell, P. B. (2000). The growth morphology and nucleation mechanism of primary L1₂ Al₃Sc particles in Al-Sc alloys. *Materials Science Forum*, 331-337, 1013-1018.
- [3] Chemingui, M., Khitouni, M., Mesmacque, G., & Kolsi, A. W. (2009). Effect of heat treatment on plasticity of Al-Zn-Mg alloy: Microstructure evolution and mechanical properties. *Physics Procedia*, 2(2), 1167-1174.
- [4] Wu, L. M., Wang, W. H., Hsu, Y. F., & Trong, S. (2008). Effects of homogenization treatment on recrystallization behaviour and dispersoid distribution in an Al-Zn-Mg-Sc-Zr alloy. *Journal of Alloys and Compounds*, 456(1), 163-169.
- [5] Nishi, M., Matsuda, K., Miura, N., Watanabe, K., Ikeno, S., Yoshida, T., *et al.* (2014). Effect of the Zn/Mg ratio on microstructure and mechanical properties in Al-Zn-Mg alloys. *Materials Science Forum*, 794-796, 479-482.
- [6] Park, J. K., & Ardell, A. J. (1983). Microstructures of the commercial 7075 Al alloy in the T651 and T7 tempers. *Metallurgical and Materials Transactions A*, 14(10), 1957-1965.
- [7] Mondolfo, L. F. (1976). *Aluminium Alloys: Structure and Properties*. Butterworth, London: Elsevier.
- [8] Shin, J., Ko, S., & Kim, K. (2012). A study on thermal conductivity and mechanical properties of Al-Zn-Mg aluminium alloys. *Materials Science Forum*, 724, 169-172.
- [9] Li, Y. Y., Wang, W. H., Hsu, Y. F., Chang, Y. L., & Trong, S. (2009). Influence of overaging on the superplastic behaviour of an Al-Zn-Mg-Zr-Sc alloy. *Materials Transactions*, 50 (3), 592-598.
- [10] John, J., Shanmughanatan, S. P., & Kiran, M. B. (2016). Friction stir welding of wrought aluminium alloys- A short review. *International Journal of Engineering Trends and Technology*, 32(2), 76-81.
- [11] Goloborodko, A., Ito, T., Yun, X., Motohashi, Y., & Itoh, G. (2004). Friction stir welding of a commercial 7075-T₆ aluminium alloy: Grain refinement, thermal stability and tensile properties. *Materials Transactions*, 45(8), 2503-2508.
- [12] Arulmoni, V. J., & Mishra, R. S. (2014). Friction stir processing of aluminium alloys for defence applications. *International Journal of Advance Research and Innovations*, 2(2), 337-341.
- [13] Venugopal, T., Rao, K. S., & Rao, K. P. (2004). Studies on friction stir welded AA 7075 aluminium alloy. *Transactions of Indian Institute of Metals*, 57(6), 659-663.
- [14] Madhusudhan, R., Sarcar, M. M. M., & Ramanaiah, N. (2013). An experimental study on mechanical and microstructural properties of dissimilar aluminium alloy friction stir welds. *International Journal of Mechanical and Production Engineering*, 1(1), 25-30.

- [15] Rhodes, C. G., Mahoney, M. W., Bingel, W. H., & Calabrese, M., (2003). Fine-grain evolution in friction-stir processed 7050 aluminium. *Scripta Materialia*, 48(10), 1451-1455.
- [16] Johannes. L. B., & Mishra R. S. (2007) Multi passes of friction stir processing for the creation of superplastic 7075 aluminium. *Materials Science and Engineering A*, 464(1), 255-260.
- [17] Kumar, N., & Mishra R. S. (2013). Ultrafine-grained Al-Mg-Sc alloy via friction-stir processing. *Metallurgical and Materials Transactions A*, 44(2), 934-945.
- [18] Mandal P. K. (2016). Experimental analysis of microstructure and mechanical behaviour in fine grained Al-Zn-Mg alloy. *International Journal of Scientific Research in Science, Engineering and Technology*, 2(1), 519-526.
- [19] Wloka, J., & Virtanen, S. (2007). Influence of scandium on the pitting behaviour of Al-Zn-Mg-Cu alloys. *Acta Materialia*, 55(19), 6666-6672.
- [20] Prabhu, T. R. (2017) Effects of ageing time on the mechanical and conductivity properties for various round bar diameters of AA 2219 Al alloy. *Engineering Science and Technology, an International Journal*, 20(1), 133-142.
- [21] Mandal P. K., & Ghosh P. K., (2014). Development of high strength Al-Zn-Mg alloys for automotive application. *Indian Foundry Journal*, 60(4), 32-39.
- [22] Werenskiold, J. C., Deschamps, A., & Brechet, Y. (2000). Characterization and modeling of precipitation kinetics in an Al-Zn-Mg alloy. *Materials Science & Engineering A*, 293(1), 267-274.
- [23] Muhammad, A., Xu, C., Wang, X. J., Hanada, S., Yamagata, H., Hao, L., *et al.* (2014). High strength aluminium cast alloy: A Sc modification of a standard Al-Si-Mg alloy. *Materials Science & Engineering A*, 604, 122-126.
- [24] Costa, S., Puga, H., Barbosa, J., Pinto, & A. M. P. (2012). The effect of Sc additions on the microstructure and age hardening behaviour of as cast Al-Sc alloys. *Materials and Design*, 42, 347-352.
- [25] Harada, Y., & Dunand, D. C.(2003). Thermal expansion of Al₃Sc and Al₃(Sc_{0.75} X_{0.25}). *Scripta Materialia*, 48(3), 219-222.
- [26] Huang, Y. C., Xiao, Z. B., & Liu, Y. (2013). Crystallography of Zr poisoning of Al-Ti-B grain refinement using edge-to-edge matching model. *Journal of Central South University*, 20(10), 2635-2642.
- [27] Tang, C., Zhou, P., Zhao, D. D., Yuan, X. M., Tang, Y., Wang, P. S., *et al.* (2012). Thermodynamic modeling of the Sc-Zn system coupled with first-principles calculation. *Journal of Mining and Metallurgy Section B: Metallurgy*, 48(1), 123-130.
- [28] Rokhlin, L. L., Dobatkina, T. V., & Korolkova, I. G. (2008). *Phase equilibria in Al-rich Al-Mg-Sc-Zn alloys at 430 and 300°C. Russia Metallurgy (Metally)*, 1, 89-92.
- [29] Isadare, A. D., Aremo, B., Adeoye, M. O., Olawale, O. J., & Shittu, M. D. (2013). Effect of heat treatment on some mechanical properties aluminium alloy. *Materials Research*, 16(1), 934-945.
- [30] Gholami, S., Emadoddin, E., Tajally, M., & Borhani, E.(2015). Friction stir processing of 7075 Al alloy and subsequent ageing treatment. *Transactions of Nonferrous Metals Society of China*, 25(9), 2847-2855.
- [31] Wang, K., Liu, F. C., Ma, Z. Y., & Zhang, F. C. (2011). Realization of exceptionally high elongation at high strain rate in a friction stir processed Al-Zn-Mg-Cu alloy with the presence of liquid phase. *Scripta Materialia*, 64(6), 572-575.
- [32] Weglowski, M., Dymek, S., S., & Hamilton, C. B. (2013). Experimental investigation and modelling of friction stir processing of cast aluminium alloy AlSi9Mg. *Bulletin of the Polish Academy of Sciences Technical Sciences*, 61(4), 893-904.
- [33] Ku, M. H., Hung, F. Y., Lui, T. S., Chen, L. H., & Chiang, W. T. (2012), Microstructure effects of Zn/Mg ratio and postheat treatment on tensile properties of friction stirred process (FSP) Al-xZn-yMg alloys. *Materials Transactions*, 53(5), 995-1001.

- [34] Feng, X., Lu, H., & Babu, S. S. (2011). Effect of grain size refinement and precipitation reactions on strengthening in friction stir processed Al-Cu alloy. *Scripta Materialia*, 65(12), 1057-1060.



P. K. Mandal was awarded his Bachelor of Engineering from the Department of Metallurgical and Materials Engineering in National Institute of Technology Karnataka (NITK), Surathkal, India. He obtained his Master of Technology from the Department of Metallurgical and Materials Engineering in Indian Institute of Technology Kharagpur (IITKgp), India. Recently, he got his Ph. D from the Department of Metallurgical and Materials Engineering in Indian Institute of Technology Roorkee (IITR), Uttarakhand in January 2017, India. The Ph.D thesis entitled “Structure-property correlation in FSPed scandium inoculated cast Al-Zn-Mg alloy”. He has published more than 20 journal papers on an international level and attended 20 national and international conferences, so far. Presently, working as an Assistant professor in Amal Jyothi college of Engineering, Kajirappally, Kerala, India. His interested areas in ferrous-nonferrous alloys development and characterizations. Also, interested in physical metallurgy, mechanical metallurgy, and nanoscience and nanotechnology related fields.